Communication

Ion–Dipole Interactions Are Asymptotically Unscreened by Water in Dipolar Nanopores, Yielding Patterned Ion Distributions

Kevin Leung

J. Am. Chem. Soc., **2008**, 130 (6), 1808-1809 • DOI: 10.1021/ja076229x

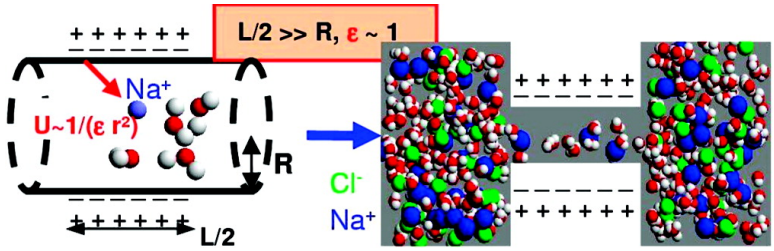

More About This Article

Additional resources and features associated with this article are available within the HTML version:

- Supporting Information
- Access to high resolution figures
- Links to articles and content related to this article
- Copyright permission to reproduce figures and/or text from this article

View the Full Text HTML

J|A|C|S
COMMUNICATIONS

Published on Web 01/18/2008

Ion−Dipole Interactions Are Asymptotically Unscreened by Water in Dipolar Nanopores, Yielding Patterned Ion Distributions

Kevin Leung

Sandia National Laboratories, MS 1415, Albuquerque, New Mexico 87185

Received September 21, 2007; E-mail: kleung@sandia.gov

Water-filled nanopores exhibit a remarkable ability to exclude or selectively transmit ions.[1−8] They have important biological functions and are potentially useful for ion current gating, desalination, and other applications. The effects of dielectric mismatch,[1] nanopore diameter,[2,4] charges,[7] and polarizability[5,9] on ion permeation and rejection have been much studied. Surprisingly, while the celebrated KcsA channel selectivity filter relies on carbonyl group dipoles pointed radially into its narrow passageway for its function,[8] dipolar decorations in synthetic nanopores have received less attention. A recent force-field-based silica nanopore model does exhibit an intrinsic preference for cations owing to an effective dipole layer on its interior surface—even at the pH of zero charge.[6] This work elucidates the dramatic effect of dipolar layers in nanopores on electrolyte permeation, which may lead to novel current−voltage ($I-V$) characteristics, and discusses pore geometries where this effect may be realized.

An infinitely long cylindrical pore of radius R_d with radially aligned surface dipoles of magnitude d and uniform surface density η_d exerts a uniform electrostatic potential $\phi_d = -4\pi\eta_d d$ in the pore interior, *independent* of R_d or the radial position of ion R. $\phi_d|e|$ is predicted to be ca. −24 kcal/mol in silica pores[6] and exceeds −100 kcal/mol inside the KcsA filter.[8,10] Here e is the electronic charge. A uniform dipole layer thus induces no electric field and does not interact with uncharged H_2O molecules. Hence its interaction with ions inside the pore is unmediated (unscreened) by the confined water. This is consistent with our hitherto puzzling observation that the free energy preference for Na^+ over Cl^- along the pore center of the infinitely long silica pore model of ref 6 is fairly independent of the presence of water. Thus, the simple uniform dipole density in our model apparently captures essential nanopore−ion interactions in nanoporous silica, where H_2O molecules do form hydrogen bonds with the surface silanol groups. This model should be pertinent to other inorganic nanopores too.

We next use two geometries to demonstrate how this intrinsic ϕ_d of dipolar nanopores may be exploited: (1) an infinitely long "tube" model, with repeating unit cells that have alternating $L/2$ long stretches in the z direction where dipole surface densities exist or vanish (Figure 1a); (2) a "membrane" geometry with dipoles in the pore interior only (Figure 1b). Regions with low local dipole density can potentially be achieved by functionalizing silica pores with amine groups.[6] Near the junction, $z = z_o$, between dipolar ($\phi = -4\pi\eta_d d$) and nondipolar ($\phi = 0$) regions, the pore-axis electrostatic potential is

$$\phi(z,R=0) = -2\pi\eta_d d\{1 + (z - z_o)R_d^{-1}/[1 + (z - z_o)^2/R_d^2]^{1/2}\} \quad (1)$$

when L far excceds $|z - z_o|$ and R_d. Figure 2a depicts $\phi(z,R)$ for $R_d = 5.5$ Å, $L = 60$ Å. $\phi(z,R)$ is fairly independent of R inside the pore but vanishes rapidly for $R > R_d$. An electric field *parallel* to the pore interior surface materializes,[11] localized within a distance R_d of the junction. This field is locally screened by water molecules.

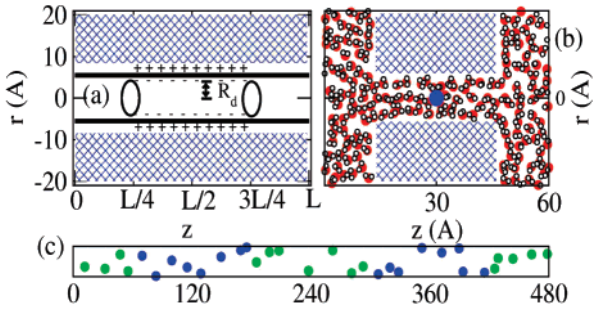

Figure 1. (a) Cylindyrical nanopore unit cell for the "tube" geometry. Ions and water are excluded from the crossed regions. Radial dipole moments (+/−) exist on alternating stretches along the pore surface. (b) "Membrane" simulation unit cell. Blue and red/white spheres depict Na^+ and H_2O, respectively. Dipoles exist on the interior pore surface only. (c) Charge segregated insulating behavior in tube geometry (see text). Na^+ and Cl^- are depicted as blue and green spheres.

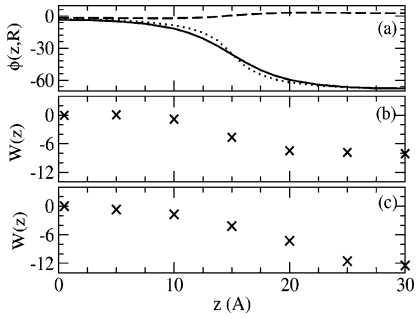

Figure 2. Na^+ potential of mean force $W(z)$ kcal/mol along the pore axis, with $\phi_d|e| = -71.7$ kcal/mol, $L = 60$ Å, and a unit cell doubled in the z-direction. (a) No water; solid, dotted, and dashed lines refer to ions at radii $R/R_d = 0$, 0.7, and 1.8, respectively. (b) Water-filled tube geometry. (c) Water-filled membrane geometry.

Note that in the membrane model, if the membrane surface has the same dipole density as the pore interior surface, it exerts an equal and opposite $\phi(z,R = 0)$ that cancels eq 1.[10] Hence, to exploit dipolar effects, the two surfaces must be functionalized differently.

To examine ion permeation into water-filled dipolar pores, we apply the atomistic H_2O, Na^+, and Cl^- force fields used in ref 6 to compute the potential of mean force, $W(z)$, for Na^+ frozen along the pore axis at different z values, using the thermodynamic integration technique.[10] Pore-water/ion interactions are described by analytical, least-square fit approximations to dipolar electrostatic and Lennard-Jones terms.[10] The pores are hydrophilic, with ∼12 Å diameter and 2.7 $Å^{-1}$ H_2O density. Infinitely long but laterally isolated tubes (Figure 1a) are simulated using at least 10^5 passes of canonical ensemble Monte Carlo (MC) runs. Membrane models (Figure 1b), periodic in all three directions with lateral unit cell lengths of 40 Å, are simulated for at least 200 ps using molecular

10.1021/ja076229x CCC: $40.75

Table 1. Na^+ Potential of Mean Force at $z = L/2$, $\Delta W_1 = W(z = L/2) - W(z = 0)$[a]

tube				membrane		
$\phi_d\|e\|$	$L/2$	ΔW_1		$\phi_d\|e\|$	$L/2$	ΔW_1
−71.7	30	−8.1		−71.7	30	−12.5
−71.7	60	−14.9		−71.7	60	−17.4
−71.7	90	−24.0		0.0	30	+3.3
−71.7	120	−32.3		0.0	60	+2.5
−23.9	60	−3.0		−23.9	30	−1.7
−23.9	120	−8.1		0.0	30	+3.3
			NaCl[b]	−71.7	30	−3.4
			NaCl[b]	0.0	30	+2.6

[a] Energies and lengths are in units of kcal/mol and Å. [b] Computed in 1.0 M NaCl electrolyte, not pure water.

dynamics (MD)/particle mesh Ewald methods. Because Na^+ orders water in nanopores in a way incompatible with the periodic boundary conditions used,[12] our simulation cells contain two unit cells doubled in the z direction for convergence.

Figure 2b depicts $W(z)$ for a $\phi_d|e| = -72$ kcal/mol and $L/2 = 30$ Å tube. The membrane geometry leads to qualitatively similar results (Figure 2c). These geometries yield $\Delta W_1 = W(L/2) - W(0) = -8.1$ and -12.5 kcal/mol. Compared with $\Delta W_1 = \phi_d|e| = -72$ kcal/mol in the absence of water, they exhibit effective dielectric constants ϵ of 8.9 and 6.0.

However, unlike transmembrane ion channels such as KcsA,[8] material pores can have lengths on the order of 1 μm. Table 1 shows that ΔW_1 in the tube geometry steadily increases with $L/2$ and is roughly proportional to ϕ_d; at $L/2 = 120$ Å, ϵ has effectively dropped to 2.3. This is readily explained as follows. Unless the localized electric field induces a ferroelectric phase transition for water (not the case here), ΔW_1 is predominantly screened by H_2O near the junctions where the electric field is at its maximum. For large L, these localized H_2O resemble a point dipole whose interaction with ions vanishes as $1/|z - z_o|^2$. Thus, the dipole layer-induced attraction for cations deep inside dipolar regions is asymptotically *unscreened* by water. ΔW_1 analysis for the membrane geometry is complicated by its nonzero value even when the dipoles are absent and by the O(1) kcal/mol statistical noise, but ΔW_1 follows a qualitatively similar trend there.

As long as $L \gg R_d$, screening should asymptotically vanish even when R_d is large. In macroscopic dipolar pore models, it will be the ever-present electrolytes in water, not water itself, that screen the ion-surface dipole interaction. Here nanoscale pores with $R_d <$ 10 Å may exhibit unique properties. (1) We consider 1.0 NaCl electrolytes in the membrane geometry. The hydration free energy of the Na^+ in the middle of the dipolar pore is reduced (last lines of Table 1) because other Na^+ ions now enter the nanopore, while Cl^- seldom do; the resulting electrostatic potential increase makes cations less favorable.[10] But unlike macroscopic pores, even the 1.0 M NaCl electrolytes do not yield complete screening in this membrane geometry. This is possibly due to confinement effects. Results from 2.7 and 5.1 ns MD trajectories with different initial configurations are averaged here because ions diffuse rather slowly. (2) Azobenzene[13] or similar functional groups can be placed at the junctions where the axial electric field is largest, further restricting water density there and hindering screening. (3) Nanopores with alternating dipolar and nondipolar surfaces may result in an ionic, charge segregated, insulating behavior.

We use MC to demonstrate that such a "phase separation" occurs with a confined 0.5 M NaCl inside an infinitely long pore with unit cell $L = 240$ Å, alternating dipolar regions, and $\phi_d|e| = -72$ kcal/mol (see Figure 1c). The effective dipole-ion screening for this L is $\epsilon = 2.3$ (Table 1). This Na^+ concentration is qualitatively consistent with our simulation of permeation of 1.0 M NaCl into the nanopore in the membrane geometry.[10] To accelerate ion sampling, water is here approximated as a continuum with $\epsilon_w = 10$.[10] We find that ion transport is blocked, even upon applying a 0.0025 V/Å electric field, screened by $\epsilon_w = 10$. We stress that this insulating behavior arises from (1) the almost-unscreened ($\epsilon = 2.3$) ion−pore dipole interaction dominating the better-screened ($\epsilon_w = 10$) ion−ion coulomb interactions, and (2) the alternating dipolar regions leading to a complete absence of cation/anion along lengths of the nanopore. Future simulations of $I-V$ characteristics, taking into account leakage of Na^+ through the nondipolar regions at long times, will be profitable.[14]

In conclusion, dipole layers naturally occur in certain nanopores, leading to intrinsic preference for cations that can be exploited when the membrane surface is functionalized differently from the pore interior or when there are alternating dipolar/nondipolar stretches inside a long pore. Our model suggests that dipole−ion interaction is asymptotically unscreened by water, leading to novel ionic, charge segregated behavior that can block ion transport and influence $I-V$ characteristics. We conjecture that dipolar nanopores may used for controlling/gating electrolyte currents instead of pores with discrete *charged* sites,[7] whose interaction with ions are much more strongly screened by water.

Acknowledgment. Sandia is a multiprogram laboratory operated by Sandia Corporation, a Lockheed Martin Company, for the U.S. Department of Energy's National Nuclear Security Administration under contract DE-AC04-94AL8500.

Supporting Information Available: Details of MD/MC models and simulations, convergence tests, and water dipole distributions. This material is available free of charge via the Internet at http://pubs.acs.org.

References

(1) Jordan, P. C. *Biophys. J.* **1982**, *39*, 157. Parsegian, A. *Nature* **1969**, *221*, 844.
(2) Beckstein, O.; Tai, K.; Sansom, M. S. P. *J. Am. Chem. Soc.* **2004**, *126*, 14694 and references therein.
(3) Kalra, A.; Garde, S.; Hummer, G. *Proc. Natl. Acad. Sci. U.S.A.* **2003**, *100*, 10175.
(4) Peter, C.; Hummer, G. *Biophy. J.* **2005**, *89*, 2222.
(5) Allen, R.; Melchionna, S.; Hansen, J. P. *J. Phys. Condens. Matter* **2003**, *15*, S297.
(6) Leung, K.; Rempe, S. B.; Lorenz, C. D. *Phys. Rev. Lett.* **2006**, *96*, 095504.
(7) Stein, D.; Kruithof, M.; Dekker, C. *Phys. Rev. Lett.* **2004**, *93*, 035901. Gracheva, M. E.; Vidal, J.; Leburton, J.-P. *Nano Lett.* **2007**, *7*, 1717. Lorenz, C. D.; Travesset, A. *Phys. Rev. E* **2007**, *75*, 061202. Goldberger, J.; Fan, R.; Yang, P. D. *Acc. Chem. Res.* **2006**, *39*, 239.
(8) Varma, S.; Rempe, S. B. *Biophys. J.* **2007**, *93*, 1093. Noskov, S. Y.; Roux, B. *J. Gen. Physiol.* **2007**, *129*, 135. Asthagiri, D.; Pratt, L. R.; Paulaitis, M. E. *J. Chem. Phys.* **2006**, *125*, 024701.
(9) Leung, K.; Marsman, M. *J. Chem. Phys.* **2007**, *127*, 154722.
(10) See Supporting Information.
(11) Bratko, D.; Daub, C.; Leung, K.; Luzar, A. *J. Am. Chem. Soc.* **2007**, *129*, 2504.
(12) Dellago, C.; Naor, M. M.; Hummer, G. *Phys. Rev. Lett.* **2003**, *90*, 105902.
(13) Liu, N. G.; Dunphy, D. R.; Atanassov, P.; Bunge, S. D.; Chen, Z.; Lopez, G. P.; Boyle, J. T.; Brinker, C. J. *Nano Lett.* **2004**, *4*, 551.
(14) Gillespie, D.; Nonner, W.; Eisenberg, R. S. *J. Phys. Condens. Matter* **2002**, *14*, 12129.

JA076229X